Plasminogen activator inhibitor-1 inhibits prostate tumor growth through endothelial apoptosis

Shang-Chiung Chen,[1] Dale O. Henry,[1] Peter R. Reczek,[2] and Michael K.K. Wong[1]

[1]Departments of Pharmacology and Molecular Therapeutics and Medicine, Roswell Park Cancer Institute, Buffalo, New York, and [2]Quintessence Biotechnology, LLC, Amherst, New York

Abstract

Plasminogen activator inhibitor-1 (PAI-1) is an important endogenous inhibitor of urokinase-type plasminogen activator. Its action in tumor angiogenesis is complicated, varying with experimental setting and its cellular origin. To further understand the mechanism of the effect of PAI-1 on tumor angiogenesis, especially newly established tumor vasculature in early tumor progression, stable transfectants (TO-PAI-1) of the human prostate adenocarcinoma, PC3, were generated in which PAI-1 expression is under the control of the tetracycline-responsive promoter (Tet-On system). The TO-PAI-1 transfectants exhibit tight inducibility of expression of biologically active PAI-1 *in vitro*. Induction of PAI-1 expression in nude mice resulted in significant inhibition of tumor growth. This inhibition appears to be due to the effect of PAI-1 on angiogenesis, because it is manifested by an initial wave of tumor endothelial apoptosis accompanied by induction of tumor cell apoptosis and inhibition of tumor cell proliferation. Similar endothelial apoptosis is observed *in vitro* when human microvascular endothelial cells are physically cocultivated with TO-PAI-1 cells on vitronectin-coated plate. Taken together, these data show for the first time that PAI-1 induces endothelial apoptosis in the newly established tumor vasculature. [Mol Cancer Ther 2008;7(5):1227–36]

Introduction

Tumor progression involves the recruitment of preexisting blood vessels, a process known as tumor angiogenesis. Angiogenesis typically induces cellular migration and tissue remodeling events involving a variety of proteases as well as protease inhibitors (1). The Plasminogen/Plasmin system is one of the most efficient enzymatic systems used by tumor and endothelial cells to break down the extracellular matrix and to invade host tissue (2–4). Urokinase-type plasminogen activator (uPA) and tissue-type plasminogen activator (tPA) both convert plasminogen to plasmin, which degrades matrix components and activates latent metalloproteinases and latent growth factors. Plasminogen activator inhibitor-1 (PAI-1) is the primary physiologic inhibitor of uPA and tPA. It not only regulates the proteolytic activity of uPA but also determines the level of uPA bound to uPA receptor by promoting the rapid endocytosis of the trimolecular uPA-PAI-1-uPA receptor complex (5, 6). PAI-1 has also been implicated in modulating cell migration via alternative mechanisms (7–9). By blocking the interaction between vitronectin, uPA receptor, and integrins, PAI-1 may induce cell detachment from the extracellular matrix and thereby interfere with cellular migration and tumor invasion.

Surprisingly, high rather than low levels of PAI-1 are predictive of poor survival prognosis for patients suffering from a variety of different cancers (10–13), and a considerable amount of data regarding the role of PAI-1 in angiogenesis and tumor growth has been obtained with diverse results (14–18). When PAI-1 was transfected into PC3 carcinoma cells and subsequent tumor growth was measured in athymic mice, it was found that the mean tumor size in PAI-1-expressing cells was significantly smaller than control tumors (14). In addition, the anti-angiogenic effect of PAI-1 has been observed in the Matrigel implant assay (18) and in the chicken chorioallantoic membrane (19). However, there are apparent discrepancies between these data and the lack of effect of PAI-1 deficiency on metastasis of melanoma cells (20), MMTV-Pym T-induced breast cancer progression (21), and the proangiogenic effect of PAI-1 observed in PAI-1-deficient mice. Taken together, these findings indicate that the role of PAI-1 as a determinant of tumor angiogenesis might vary with experiment settings (tumor-type or injection site dependent) and might depend on its cellular origin (tumor cells versus host cells) as well as dosage.

However, most of the studies involved in implanting tumor cells, constitutively PAI-1-expressing cells, PAI-1-containing Matrigel, or aortic ring explant into PAI-1-deficient or wild-type immunocompromised mice. As a result, the effects of PAI-1 before the initial formation of vasculature were obtained. Recently, several studies have indicated the differential efficacies of angiogenic inhibitors depending on the stage of carcinogenesis as well as angiogenesis (22, 23). Angiogenic inhibitors, such as angiostatin and endostatin, are more potent in the early stage of tumorigenesis than in the late stage of tumorigenesis or before initial formation of the vasculature. Similar to angiogenic inhibitors, a stage-specific effect has also been

Received 1/22/08; revised 3/5/08; accepted 3/6/08.

Grant support: Department of Medicine Development Funds.

The costs of publication of this article were defrayed in part by the payment of page charges. This article must therefore be hereby marked *advertisement* in accordance with 18 U.S.C. Section 1734 solely to indicate this fact.

Requests for reprints: Michael K.K. Wong, Departments of Pharmacology and Molecular Therapeutics and Medicine, Roswell Park Cancer Institute, Elm & Carlton Streets, Buffalo, NY 14263.
Phone: 716-845-7611; Fax: 716-845-4542.
E-mail: Michael.Wong@RoswellPark.org

doi:10.1158/1535-7163.MCT-08-0051

shown with several proangiogenic factors, such as fibroblast growth factor-2 and vascular endothelial growth factor (24, 25). Conditional down-regulation of fibroblast growth factor-2 or vascular endothelial growth factor expression in xenografts with 200 to 300 mm^3 caused a significant decrease in tumor growth. In contrast, late down-regulation of fibroblast growth factor-2 or vascular endothelial growth factor protein expression did not affect the further growth of the lesion.

In an attempt to investigate the effect of PAI-1 on established tumor vasculature in the early stage of tumor progression, we have created a stable PC3 Tet-On cell line. The expression of PAI-1 was induced by administrating tetracycline derivatives such as doxycycline when xenografts reached 300 mm^3. Tumorigenicity and angiogenic phenotype were compared in tumors harvested from different time points. Our results showed the inhibition of tumorigenesis and angiogenesis by PAI-1, which is accompanied by an increase of endothelial apoptosis after PAI-1 induction.

Materials and Methods

Reagents

Recombinant human PAI-1 was purchased from Molecular Innovations. Mouse monoclonal anti-PAI-1 antibody was from Santa Cruz Biotechnology. Rabbit polyclonal antibody to cleaved caspase-3 was from Cell Signaling Technology. Mouse monoclonal antibody to human CD31 and rat anti-mouse CD31 were purchased from DAKOCytomation and BD PharMingen, respectively. Doxycycline was from Sigma-Aldrich.

Cell Culture and Transfection

Human prostate adenocarcinoma cell line PC3 was obtained from American Type Culture Collection and cultured in F12K (Invitrogen) supplemented with 10% Tet System Approved FBS (BD Biosciences), 100 μg/mL streptomycin, and 100 unit/mL penicillin at 37°C in a 5% CO_2 atmosphere.

To generate tetracycline (or doxycycline)–responsive PAI-1 and enhanced green fluorescent protein (GFP) transfectants, human PAI-1 cDNA fragment (generous gift from Dr. Daniel Lawrence; 1,736 bp) and enhanced GFP cDNA fragment (730 bp cut from pEGFP-C1; BD Biosciences) were subcloned into the *Bam*HI- and *Xba*I-digested pcDNA4/TO vector (Invitrogen) to give conditional expression vectors pTO-PAI-1 and pTO-GFP, respectively. The orientations and sequences were confirmed by nucleotide sequencing. When PC3 cells were 90% to 95% confluent after being plated at 5×10^5 per well on six-well plates, they were first transfected with 2 μg pcDNA6-TR plasmid (Invitrogen) using 4 μL LipofectAMINE (Invitrogen) in serum-free F12K following manufacturer's protocol. After 6 h of incubation, the medium was changed to complete F12K medium, and the cells were passaged into complete F12K medium containing 5 μg/mL blasticidin. After incubation for 14 days, the resulting colonies were expanded under blasticidin selection and then transfected with either pTO-EGFP or pTO-PAI-1. Zeocin (50 μg/mL) were added to the culture medium 48 h after transfection. After 3 weeks of selective pressure, the Zeocin-resistant clones (TO-EGFP and TO-PAI-1 cells, respectively) were isolated, expanded, and tested for doxycycline responsiveness.

PAI-1 Protein Production by TO-PAI-1 Transfectants

Transfectants were grown to 70% confluence. Then, cells were incubated in fresh serum-free medium for 2 days in the presence or absence of 1 μg/mL doxycycline. Conditioned media were collected. Monolayers were washed three times with ice-cold PBS, dissolved in lysis buffer (CelLytic-M, Sigma), and collected. After centrifugation at 12,000 rpm at 4°C for 20 min, supernatants were then collected as cell extracts.

For immunoblot analysis, collected conditional media were incubated with 0.5 mL heparin-Sepharose bead slurry (Bio-Rad Laboratories) at 4°C for at least 4 h in a tube rotator. The beads were then precipitated by centrifugation at 4°C for 10 min. After removing the supernatant, the beads were washed twice with 5 mL ice-cold PBS, resuspended in 50 μL of 2× Laemmli buffer [0.5 mol/L Tris-HCl (pH 6.8), 5% β-mercaptoethanol, 0.1% (w/v) bromophenol blue, 20% (v/v) glycerol], and boiled for 5 min. Samples were run on 10% SDS-PAGE, and protein were electrophoretically transferred to polyvinylidene fluoride membranes in 20% methanol, 190 mmol/L glycine, and 25 mmol/L Tris-HCl. After transfer, membranes were blocked with 5% skim milk in PBS/0.05% Tween 20 at room temperature for 1 h and probed with anti-PAI-1 antibody diluted 1:1,000 in PBS/0.05% Tween 20. Immunocomplexes were visualized by Alexa Fluor 680–conjugated secondary antibodies (Invitrogen) and the Odyssey Infrared Imaging System (LI-COR).

ELISA

PAI-1 level of cell extracts was determined by IMUBIND Plasma PAI-1 ELISA (American Diagnostica) in accordance with manufacturer's instructions. The absorbance of the wells was measured on a SpectraMax Plus^{384} ELISA plate reader (Molecular Devices), and the standard curves were drawn through absorbance values of standard solutions.

To examine vitronectin-binding activity, 96-well non-tissue culture-treated plates were coated with 100 μL/well of 2 μg/mL native vitronectin (Molecular Innovations) at 4°C overnight. Nonspecific binding was blocked with 3% bovine serum albumin for 1 h at 37°C. Cell extracts (50 μg) were then added and incubated at room temperature for 1 h. Following incubation, cell extracts were removed, wells were washed, and bound PAI-1 was detected by using monoclonal anti-PAI-1 antibody and peroxidase-conjugated anti-mouse IgG. The plates were then developed with SureBlue TBS Microwell Peroxidase Substrate (KPL) and read (λ = 450 nm) on ELISA plate reader.

To examine protease-inhibitory activity, similar assays were done on urokinase-coated plate (Molecular Innovations).

MTS Assay

Cell viability was assessed by MTS assay (CellTiter 96 AQueous One Solution Cell Proliferation Assay; Promega). Briefly, 1,000 cells of TO-PAI-1, TO-GFP, and parental PC3

cells were seeded in 96-well plate after the second subculture. Cells were incubated in the presence or absence of 1 μg/mL doxycycline at 37°C. At the end of incubation, 20 μL CellTiter 96 AQueous One Solution reagent containing tetrazolium compound (MTS) were added to each well and the cells were incubated for 2 h at 37°C. Afterwards, optical absorbance was determined at 490 nm according to manufacturer's manual.

Tumorigenicity Assay

Female 6- to 8-week-old NCr-*nu/nu* mice were obtained from the animal production colony of the National Cancer Institute, Frederick Cancer Research and Development Center. Cells were harvested by brief exposure to 0.25% trypsin/0.02% EDTA, washed twice, suspended in serum-free RPMI 1640/Matrigel mixture (1:1), and injected into the left flank region (2×10^6 cells per mouse). The tumor volume was measured twice a week with calipers, and tumor weight was estimated by the formula: (length × width^2) / 2. When tumor volume is at least 300 mm^3, mice were fed with water containing 2 mg/mL doxycycline and 5% (w/v) sucrose (26) to induce the expression of tumor transgenes. Based on the study by Hebda et al. (27), this doxycycline concentration does not affect normal angiogenesis, matrix metalloproteinase activity, collagen synthesis, or wound healing. At different time points, animals were sacrificed, sera were collected, and tumors were harvested and processed for PAI-1 antigen analysis and immunohistochemical staining.

Immunohistochemical Staining

Formalin-fixed tumor tissue were immunoperoxidase stained for PAI-1 (Molecular Innovations), CD31 (BD PharMingen), cleaved-caspase-3 (Cell Signaling Technology), and Ki-67 (Neomarker) by the Roswell Park Cancer Institute Histology Core Facility. Briefly, tumor sections were cut into 5 μm sections, placed on charged slides, and dried in a 60°C oven for 1 h. After deparaffinization and rehydration of tumor sections, endogenous peroxidase was quenched with aqueous 3% H_2O_2. Antigen retrieval was done with citrate buffer (pH 6.0) in the microwave for 10 min followed by PBS/T wash. Sections were then treated with protein-blocking solution (0.03% casein in PBS/T) for 30 min and the primary antibody was applied for 60 min at room temperature. After incubation of biotinylated secondary antibody for 30 min, Zymed streptavidin was applied for 30 min. Signals were then developed with DAKO DAB Chromagen followed by hematoxylin counterstain.

For double immunostaining, the described protocol was followed to detect cleaved caspase-3. Subsequently, the sections were washed three times in PBS/T, and the same protocol was repeated, staining for CD31, which was developed with streptavidin-biotin conjugated to alkaline phosphatase and counterstained with Fast Red.

Assessment of Microvessel Density

Mean microvessel density was assessed according to Weidner et al. (28). Briefly, the sections will be scanned at low magnifications (×25 and ×100) to identify the most vascular areas of the tumor (hotspots). Within these areas, mostly localized in the periphery of the lesion, a maximum of 10 fields at ×400 magnification are examined, and the mean value of these field calculated.

Image Analysis

Quantitative analysis of immunohistochemically stained sections were done using ImageJ software (version 1.37v; NIH; ref. 29). Digitized images were captured at ×100 magnification, three different fields per stained section. Each image was split into its component red, green, and blue colors. The three images were then converted to grayscale images. The total number of cells was counted in the red image, and the number of immunohistochemically positive cells was counted in the blue image. A threshold was set for clear visualization of the displayed image.

Flow Cytometric Apoptosis Analysis

Cells of TO-PAI-1 (2×10^3) were first seeded on sterile vitronectin-coated glass coverslips and grown in 300 μL EGM-2 MV medium (Clonetics) in the presence or absence of 1 μg/mL doxycycline for 24 h. A suspension of HMEC-1 was then added to coverslips (2×10^3 cells per coverslip), and TO-PAI-1 and HMEC-1 were cocultivated at 37°C in the presence or absence of 1 μg/mL doxycycline for 48 h. Control experiments were done with HMEC-1 cultured in the presence of 1 nmol/L paclitaxel (positive) or 1 μg/mL doxycycline (negative). After the incubation period, cells were trypsinized, harvested by centrifugation at 1,000 × *g* for 10 min, repeatedly washed with ice-cold PBS, and then suspended in ice-cold binding buffer [10 mmol/L HEPES/NaOH (pH 7.4), 140 mmol/L NaCl, 2.5 mmol/L $CaCl_2$]. The rate of endothelial apoptotic cells was quantified using Annexin V-PE Apoptotic Detection Kit (BD PharMingen) combined with APC-conjugated anti-human CD31 (eBioscience). Because Annexin V may also bind to necrotic cells, counterstaining with 7-AAD was done to discriminate between necrotic and apoptotic cells. Cells were incubated for 15 min at room temperature. Cell suspensions were evaluated by a FACSCalibur system (Becton Dickinson) with gate analysis method to discriminate endothelial cells for further apoptosis analysis. Results were expressed as the number of apoptotic cells per 100 cells (%) with 10,000 cells counted.

Results

Conditional PAI-1 Expression in TO-PAI-1 Cells Is Tightly Regulated by Doxycycline

Human prostate adenocarcinoma cells, PC3, containing a tetracycline-inducible cassette for conditional PAI-1 or GFP expression (TO-PAI-1 and TO-GFP, respectively) were established. Doxycycline, a stable derivative of tetracycline, was used to modulate transgene expression.

In the absence of doxycycline, TO-PAI-1, TO-GFP, and parental PC3 cells all express negligible levels of PAI-1 as determined by PAI-1 ELISA on cell extracts (Fig. 1A, *solid column*). In the presence of doxycycline (Fig. 1A, *open column*), a dramatic increase of PAI-1 expression was seen in TO-PAI-1 cells (349.09 ± 4.5 ng/mg) when compared with control TO-GFP (52.62 ± 1.73 ng/mg) or parental PC3 cells (50.12 ± 1.89 ng/mg). PAI-1 is a secreted protein, and

examination of the supernatants by immunoblotting likewise shows similar tight inducibility of PAI-1 expression in TO-PAI-1 cells (Fig. 1A, *inset*). Fluorescence microscopy of control TO-GFP cells showed similar levels of inducibility compared with TO-PAI-1 cells (data not shown), showing the feasibility of using GFP as a control for transfection as well as transgene induction *in vitro* and *in vivo*. Dose-response experiments show that the maximal induction of expression in TO-GFP and TO-PAI-1 is obtained at doxycycline doses of ≥100 ng/mL. Induction is readily evident at 24 h post-doxycycline and is maximal (>95% induction) by 48 h (data not shown).

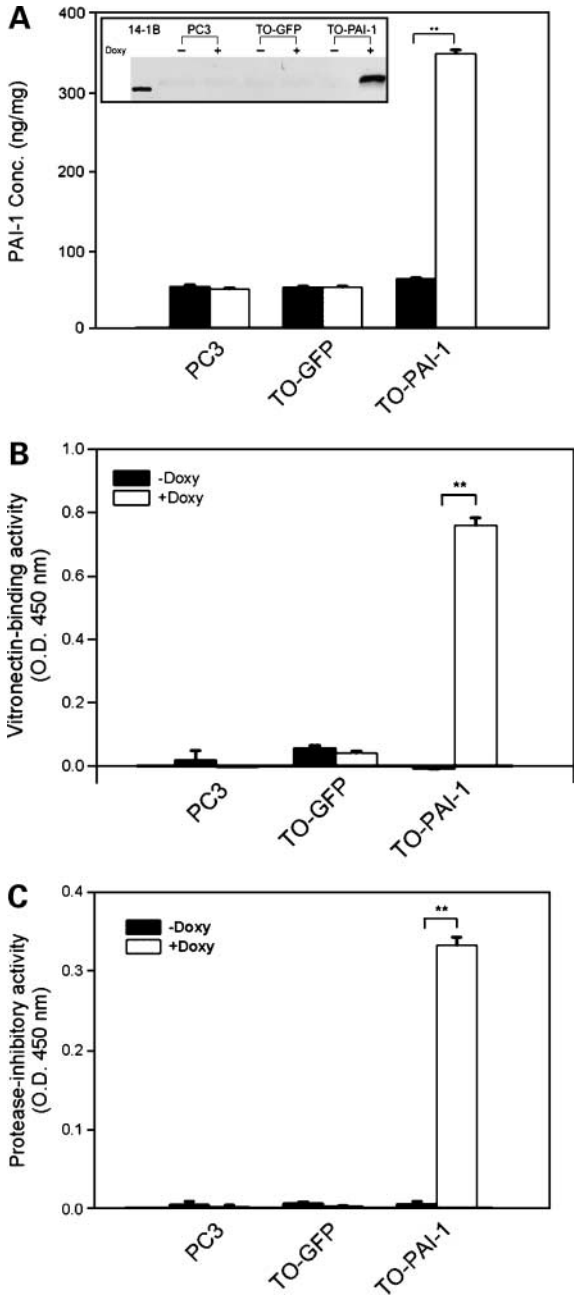

Figure 1. Conditional PAI-1 expression in TO-PAI-1 cells is tightly regulated by doxycycline. Parental PC3 cells, TO-GFP, and TO-PAI-1 transfectants were grown for 2 days in the presence (*open column*) or absence (*solid column*) of 1 μg/mL doxycycline. Expression of PAI-1 was analyzed by PAI-1 ELISA of cell lysate (**A**) and immunoblotting of conditioned medium (**A**, *inset*). Cell lysates were also evaluated for the activity of vitronectin binding (**B**) and protease inhibition (**C**) as described in Materials and Methods. Mean ± SE of two experiments in triplicate. **, $P < 0.01$, statistically different from the cell lysate of corresponding doxycycline-untreated cells (Student's *t* test).

PAI-1 possesses two distinct biological activities, vitronectin binding and protease inhibition. To assess whether PAI-1 produced by TO-PAI-1 cells has these same activities, cell extracts were obtained and assayed for vitronectin-binding and protease-inhibitory functions *in vitro*. As shown in Fig. 1B and C, only doxycycline-treated TO-PAI-1 cells possessed significant vitronectin-binding and protease-inhibitory activities when compared with untreated cells. None of these activities were observed in the parental PC3 cells or in the TO-GFP transfection control cells.

The MTS assay was done to evaluate the effect of PAI-1 expression on cell growth. The *in vitro* growth rate of TO-PAI-1 transfectants is identical to that of TO-GFP or parental PC3 cells and was independent of doxycycline. In addition, no morphologic differences were apparent between these cell lines (data not shown). Transfectants containing doxycycline-inducible PAI-1 were subsequently used to evaluate PAI-1 activity on PC3 tumor growth *in vivo*.

In vivo Induction of Xenograft Tumor PAI-1 Results in Tumor Growth Inhibition

Because PAI-1 is inducible and functional, determined by vitronectin binding and protease inhibition, in TO-PAI-1 cells, and because doxycycline did not affect the growth rate, the cells described were ideal for *in vivo* studies of the effects of PAI-1 on tumor growth. Hence, 2×10^6 TO-PAI-1 cells were implanted s.c. into the flank of nude mice (15 animals per group) and their growth rate was monitored. Each of the implanted cell lines grow at a similar rate *in vivo* as determined by gross examination and measurement of tumor volume. The median time to reach 200 mm^3 tumor volume is 50 days for control TO-GFP xenografts and 52 days for TO-PAI-1. When tumor volume reached 300 mm^3 at ~58 days, doxycycline-doped drinking water was given to induce transgene expression. Five animals of each group were sacrificed at three different time points, representing pre-doxycycline, 2 days post-doxycycline, and 21 days post-doxycycline induction (Fig. 2, *black arrows*). Xenografted tumors derived from TO-PAI-1 cells show a dramatic retardation in tumor growth when compared with those derived from TO-GFP cells (Fig. 2). The induction of PAI-1 expression was confirmed by direct visualization using anti-PAI-1 immunohistochemistry (Fig. 2, *inset*) and PAI-1 ELISA (Table 1). No PAI-1 is detected in naive or doxycycline-treated TO-GFP tumor tissue. Tumor extracts from doxycycline-treated animals showed an increase of PAI-1 concentration in the TO-PAI-1 group as early as 2 days post-doxycycline treatment (Table 1), and this elevation persisted for at least 21 days of continuous doxycycline treatment. In contrast, there is no significant

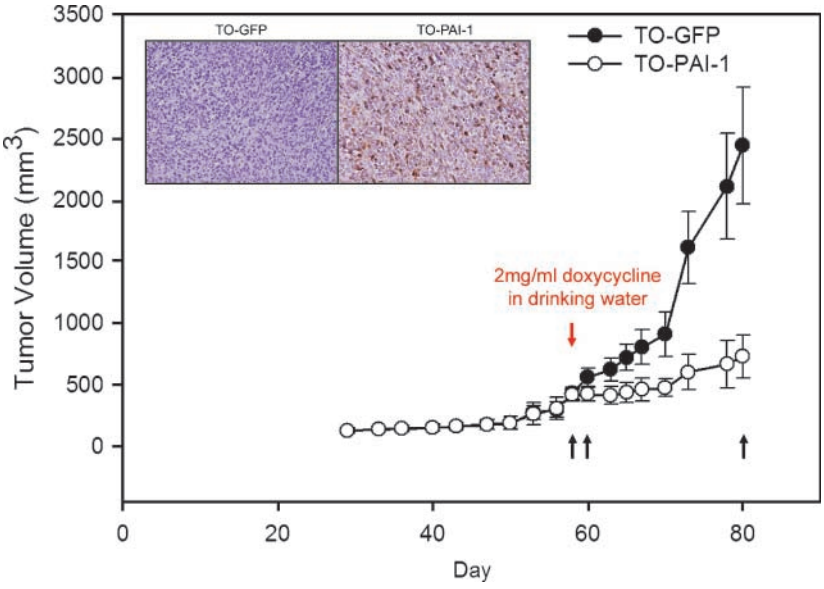

Figure 2. *In vivo* induction of PAI-1 expression results in tumor growth inhibition. Nude mice were transplanted by s.c. injection of 2×10^6 TO-GFP (●) or TO-PAI-1 (○) cells. Tumors were allowed to reach a volume of 300 mm^3 before treatment. Doxycycline (2 mg/mL) was then added in the drinking water (*red arrow*) to induce PAI-1 expression. Confirmation of induction is by PAI-1 immunohistochemical staining (*inset*). Animals were sacrificed at three time points (*black arrows*).

change of PAI-1 levels in the TO-GFP group compared with untreated animals from either TO-GFP or TO-PAI-1 group. The sera of doxycycline-treated animals from either TO-GFP or TO-PAI-1 group show similar baseline PAI-1 levels, 0.75 ± 0.04 and 0.74 ± 0.05 ng/mL, respectively, which is at the lower limit of detection for this assay. This suggests that despite the overt presence of PAI-1 within tumor tissue no detectable amount leaves the tumor compartment.

PAI-1 Induction Results in the Selective Loss of Angiogenic Microvasculature

Xenografted tumors harvested at each time point were assessed by determining the density of immunohistochemically stained $CD31^+$ blood vessels within the tumors. Both TO-GFP and TO-PAI-1 tumors show comparable vascular morphology and architecture (Fig. 3A) as well as vascular density (Fig. 3B) at the pre-doxycycline and 2 days post-doxycycline time points. PAI-1 overexpression leads to a significantly lower microvascular density (40.2 ± 6.5 blood vessels per ×100 field) compared with control GFP-overexpressing tumors at the 21 days post-doxycycline time point (95.0 ± 8.1 blood vessels per ×100 field). Striking differences in the morphology and architecture of $CD31^+$ vessels are also evident when TO-PAI-1 tumors are compared with control TO-GFP tumors at the 21 days post-doxycycline time point (Fig. 3A). Whereas the microvasculature of TO-PAI-1 tumors examined show a large number of relatively homogeneous small-caliber vessels, TO-GFP tumors exhibit a richly arborized, heterogeneous network of microvessels that successively branch from larger vessels.

Table 1. PAI-1 concentration in tumor extracts (ng/mg total protein)

	TO-GFP	TO-PAI-1
Pre-doxy	60.2 ± 5.5	64.0 ± 6.0
2 d Post-doxy	62.1 ± 6.2	397.7 ± 64.7
21 d Post-doxy	59.4 ± 6.8	473.6 ± 65.5

PAI-1 Induction Results in Rapid Endothelial Apoptosis *In vivo*

To elucidate the possible mechanisms of PAI-1-mediated antiangiogenesis, the effect of PAI-1 on endothelial cell apoptosis *in vivo* was determined. The microvessel density between TO-PAI-1 and TO-GFP xenografts are similar just before doxycycline induction (66.5 ± 12.2 and 67.2 ± 6.7 blood vessels per ×100 field, respectively). In addition, endothelial apoptosis is negligible within both groups at this time point (Fig. 4A). A wave of endothelial apoptosis occurs within the TO-PAI-1 tumors at 2 days after doxycycline treatment (10.2 ± 1.5% apoptotic endothelial cell per ×100 field) despite comparable microvessel density between TO-GFP and TO-PAI-1 tumors (Fig. 3B). In contrast, no significant change in endothelial apoptosis within control TO-GFP tumors was detected (0.8 ± 0.8% apoptotic endothelial cell per ×100 field; Fig. 4A). The dramatic elevation of endothelial apoptosis in TO-PAI-1 tumors was greatly reduced by 21 days post-doxycycline (2.6 ± 0.9% apoptotic endothelial cell per ×100 field) despite a negligible increase in endothelial apoptosis when compared to TO-GFP tumors (0.8 ± 0.8% apoptotic endothelial cell per ×100 field).

Quantification of tumor cell apoptosis was done to determine whether increased endothelial apoptosis post-PAI-1 induction is correlated with alteration in levels of intratumoral apoptosis (Fig. 4B). TO-GFP and TO-PAI-1 tumors exhibited comparable apoptotic index before doxycycline treatment (1.5 ± 0.2% and 1.4 ± 0.1% apoptotic tumor cell per ×100 field, respectively). An increase of tumor cell death was observed in TO-PAI-1 tumors (2.4 ± 0.1% apoptotic tumor cell per ×100 field) at 2 days post-doxycycline

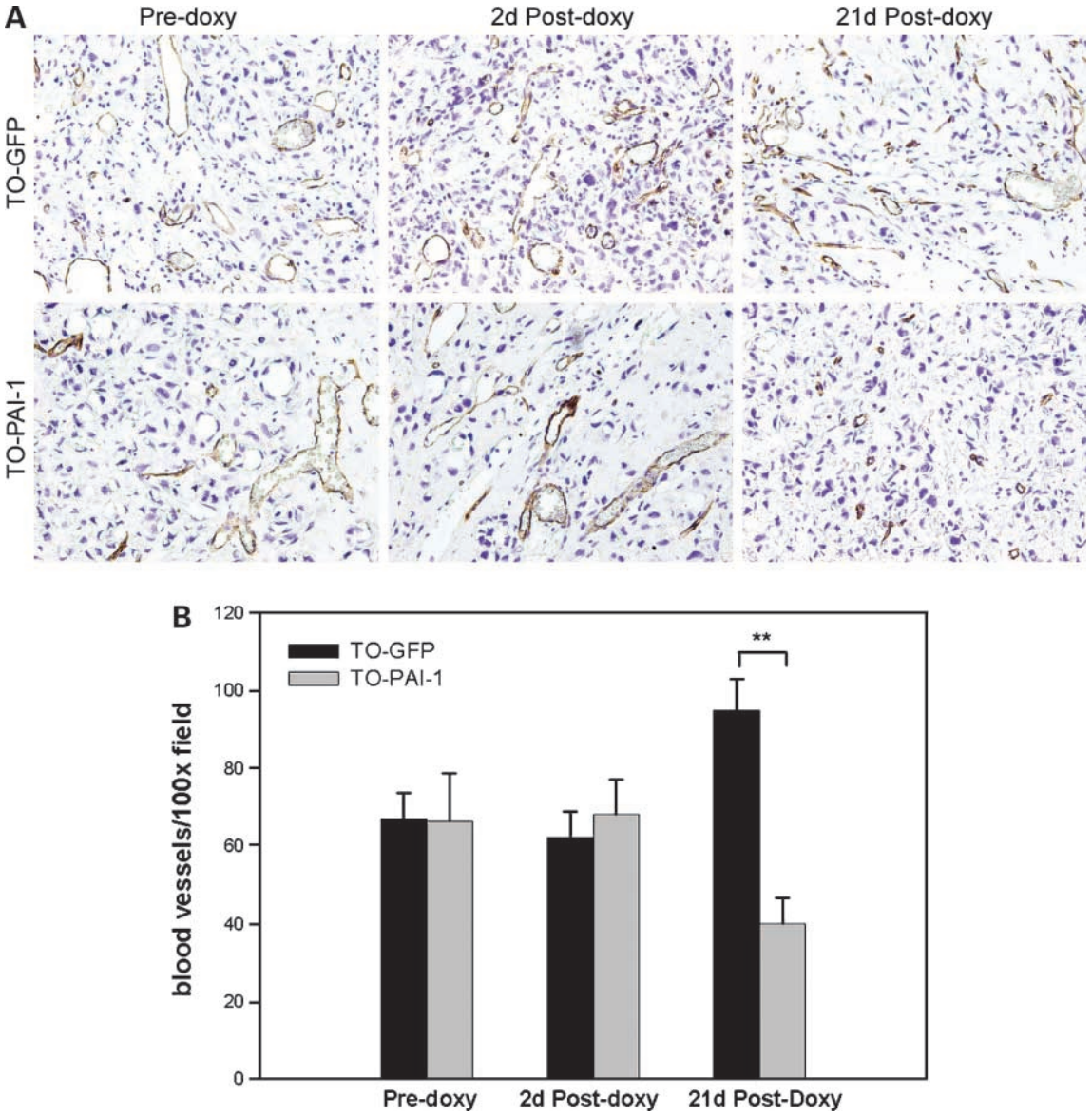

Figure 3. *In vivo* induction of PAI-1 expression results in angiogenesis inhibition. Tumor sections were processed for CD31 immunohistochemical staining. **A,** representative CD31 immunostained TO-GFP and TO-PAI-1 tumor sections at three time points. **B,** quantitation of microvessel density. Mean ± SD of five different fields of five tumor sections. **, $P < 0.01$, statistically different from corresponding TO-GFP tumor sections (Student's *t* test).

treatment in comparison with TO-GFP (1.6 ± 0.1% apoptotic tumor cell per ×100 field). The elevation of tumor cell death in TO-PAI-1 tumors was diminished (1.9 ± 0.1% apoptotic tumor cell per ×100 field) at 21 days post-doxycycline time point. Interestingly, a significant increase of tumor cell apoptosis was observed in TO-GFP tumors at this time point (2.7 ± 0.1% apoptotic tumor cell per ×100 field).

Tumor cell proliferation was also analyzed by immunohistochemical staining for Ki-67 antigen (Fig. 4C). Tumor cell proliferation is almost identical between TO-PAI-1 and TO-GFP tumors (58.4 ± 4.6% and 60.5 ± 8.0% Ki-67-positive tumor cell per ×100 field, respectively) just before doxycycline induction. However, there is a significant decrease in tumor cell proliferation occurring concomitantly with the initial wave of endothelial cell death in the TO-PAI-1 tumors (28.5 ± 3.6% Ki-67-positive tumor cell per ×100 field). In contrast, this does not change within the control TO-GFP tumors at the 2 days post-doxycycline (61.0 ± 4.6% Ki-67-positive tumor cell per ×100 field). This difference in proliferation between the control TO-GFP and the TO-PAI-1 tumors persists out to day 21.

Tumor growth is the balance between cell proliferation and apoptosis, and as such, the ratio between Ki-67-positive cells and apoptotic cells was examined. TO-GFP and TO-PAI-1 tumors exhibited comparable ratio of

Ki-67-positive cell/apoptotic tumor cell before doxycycline treatment (42.0 ± 2.3 and 41.6 ± 1.2, respectively). Consistent with the initial wave of endothelial cell death in the TO-PAI-1 tumors, a reduction of Ki-67-positive cell/apoptotic tumor cell ratio was observed in TO-PAI-1 tumors (11.8 ± 0.2) at 2 days post-doxycycline treatment in comparison with TO-GFP (38.1 ± 2.4). The dramatic reduction of Ki-67-positive cell/apoptotic tumor cell ratio in TO-PAI-1 tumors was greatly decreased by 21 days post-doxycycline (17.6 ± 0.5) despite a significant difference is still manifested when compared with TO-GFP tumors (22.5 ± 0.5).

PAI-1 Induces Vitronectin-Dependent Endothelial Apoptosis *In vitro*

Previous studies have shown that the modulation of cell adhesion to vitronectin by PAI-1 and this adhesion-inhibitory effect may lead to increased cell apoptosis. To test if the observed induction of endothelial apoptosis by PAI-1 is vitronectin dependent, cocultivation of doxycycline-treated TO-PAI-1 cells with microvascular endothelial cells (HMEC-1) on vitronectin-coated or vitronectin-uncoated plate was done. Apoptosis is evident in HMEC-1 cells when incubated alone with paclitaxel as positive control on vitronectin-coated (6.8 ± 0.4%) or vitronectin-uncoated plates (6.0 ± 0.3%). However, when incubating HMEC-1 cells alone with doxycycline, there is no significant apoptosis induction observed on either vitronectin-coated (1.1 ± 0.5%) or vitronectin-uncoated plates (1.1 ± 0.2%). This indicates the absence of effect of doxycycline on HMEC-1 apoptosis. When cocultivating with TO-PAI-1 cells on vitronectin-coated plate, HMEC-1 cells showed a significant induction of endothelial apoptosis in the presence of doxycycline (3.8 ± 0.2%) but not in the absence of doxycycline (0.6 ± 0.3%; Fig. 5). The induction

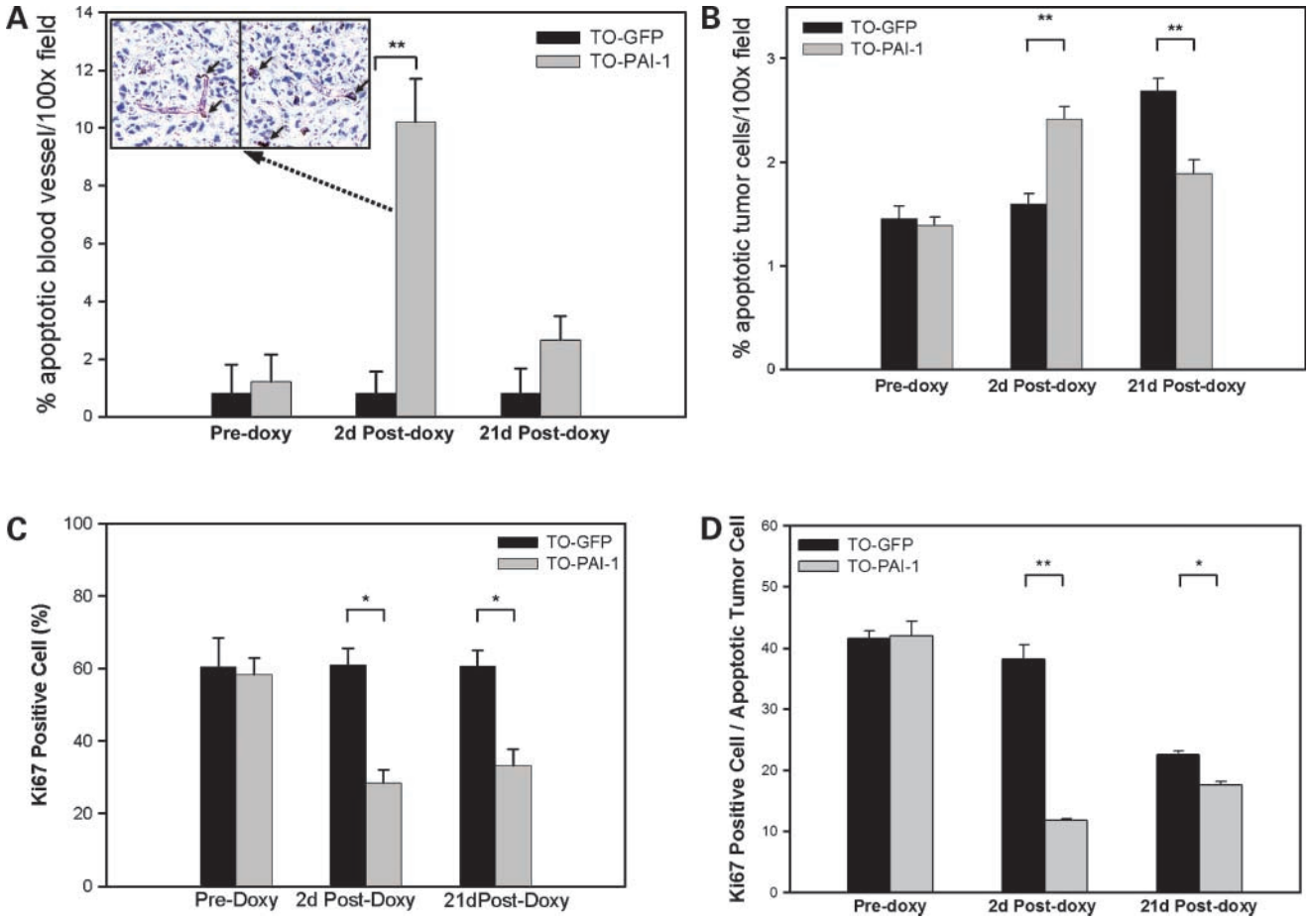

Figure 4. PAI-1 induction results in an initial wave of endothelial apoptosis. Tumor sections from each time point were subject to CD31/cleaved caspase-3 (**A** and **B**) or Ki-67 (**C**) immunohistochemical staining and quantified as described in Materials and Methods. **A,** percentage of CD31/cleaved caspase-3 double-positive blood vessel. Mean ± SD of five different fields of five tumor sections. Two representative CD31/cleaved caspase-3 immunostained TO-PAI-1 tumor sections at 2 d post-doxycycline time point (*inset*) and the CD31/cleaved caspase-3 double-positive cells (*black arrows*). **B,** percentage of cleaved caspase-3-positive tumor cells. Mean ± SD of five different fields of five tumor sections. **C,** percentage of Ki-67-positive cell. Mean ± SD of three different fields of five tumor sections. **D,** ratio between Ki-67-positive cell and apoptotic tumor cell. Mean ± SD of three different fields of five tumor sections. *, $P < 0.05$, statistically different from corresponding TO-GFP tumor sections (Student's *t* test); **, $P < 0.01$, statistically different from corresponding TO-GFP tumor sections (Student's *t* test).

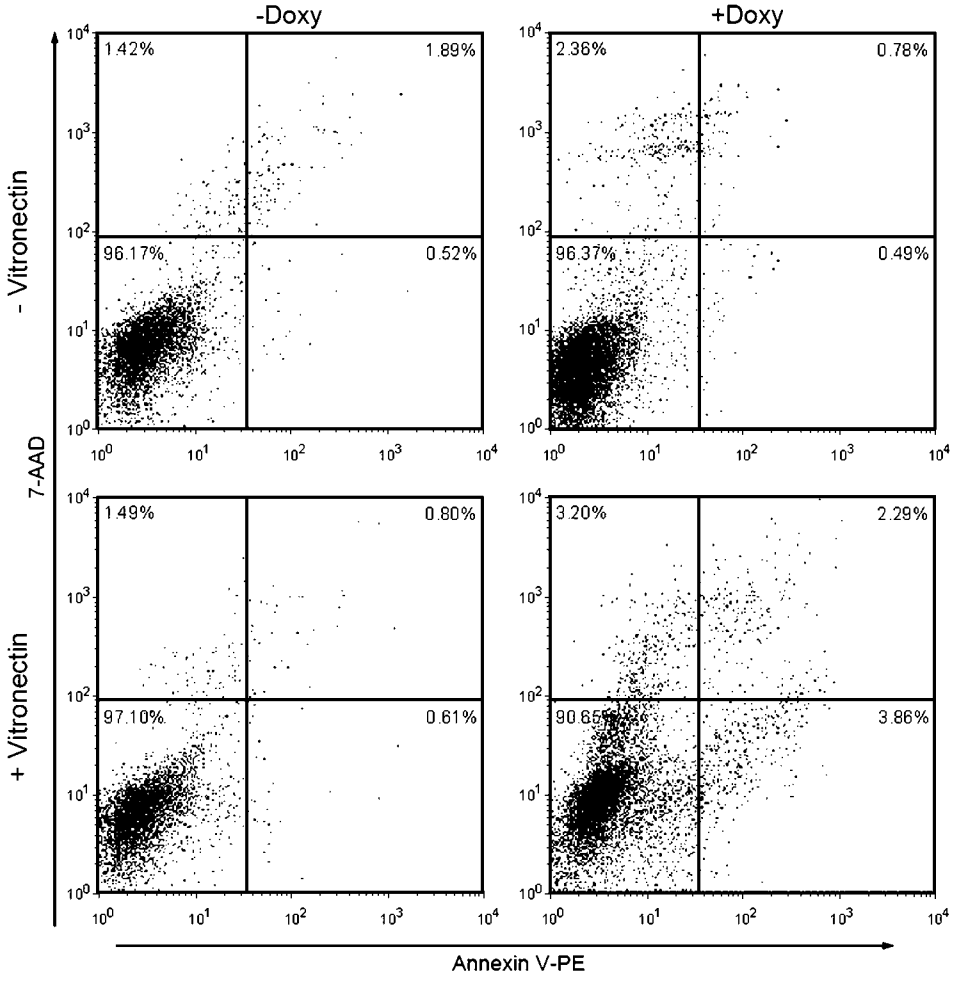

Figure 5. Coculture of TO-PAI-1 with HMEC-1 results in increased apoptosis in HMEC-1 cells. TO-PAI-1 cells were cocultured with HMEC-1 cells in EGM-2 MV medium on vitronectin-coated or vitronectin-uncoated tissue culture plate. Fluorescence-activated cell sorting analysis was done after staining with Annexin V-PE/7-AAD and APC-conjugated anti-human CD31 antibody. $CD31^+$ cells were gated for further apoptosis analysis.

of endothelial apoptosis was not observed in the absence of vitronectin in both the presence and the absence of doxycycline (Fig. 5), nor when HMEC-1 cells were cocultivated with TO-GFP in all conditions (data not shown). These data suggest that the induction of endothelial apoptosis by PAI-1 is vitronectin dependent.

Discussion

The role of PAI-1 in angiogenesis is controversial with both inhibitory and promoting effects described in previous studies. These conflicting results may arise because of differences in tumor models, differences in the source of PAI-1 (tumor cells versus host cells), or its anatomical location. To further explore the effects of PAI-1 on newly established tumor vasculature, human prostate adenocarcinoma cells, PC3, conditionally expressing PAI-1 or GFP were established. Both TO-PAI-1 and TO-GFP show doxycycline-dependent induction of transgene expression as shown by PAI-1 ELISA and immunoblotting for TO-PAI-1 (Fig. 1A) and fluorescence microscopy for TO-GFP (data not shown). Previous studies by Kwaan et al. has established several PC3 cell lines constitutively expressing PAI-1 with levels in cell extracts ranging from 13 to 18 ng per 10^6 cells per 24 h (14). Primary xenografted tumors derived from these cell lines exhibited reduced tumor volume as well as density of tumor-associated vasculature. In the current study, TO-PAI-1 cells were cultured in the presence of doxycycline for 2 days. Given an input of $\sim 6 \times 10^6$ cells, PAI-1 levels in cell extracts would produce $\sim$30 ng per 10^6 cells per 24 h. This indicates that TO-PAI-1 cells, when induced by doxycycline, express comparable PAI-1 levels to stably PAI-1-transfected PC3 cell lines described in previous study (14). At the same time, the induced TO-PAI-1 cells show no notable difference in cell growth when compared with naive TO-PAI-1, TO-GFP, or parental PC3 cells.

When injected s.c. in nude mice, both TO-PAI-1 and TO-GFP cells produce tumors that grow at a rate similar to parental PC3 cells (Fig. 2; data not shown). Doxycycline administration in the drinking water after tumor size reaches 300 mm^3 caused a significant decrease in the growth rate of TO-PAI-1 xenografts compared with that of TO-GFP xenografts (Fig. 2). These results are in accordance with results from Soff et al. (14) and Jankun et al. (30), where endogenous and exogenous PAI-1 significantly

inhibits tumor growth. This inhibition is largely attributed to the antiangiogenic effect of PAI-1 as shown by CD31 immunohistochemical staining (Fig. 3) and previous studies (18).

Interestingly, a wave of tumor endothelial apoptosis 2 days post-PAI-1 induction was observed (Fig. 4A). Previous studies show that PAI-1 inhibits endothelial cell adhesion and migration on vitronectin (31). Vitronectin is specifically present around microvessels (19, 31) and may serve as the adhesion molecular for endothelial cells during angiogenic response. The results described here support a model in which PAI-1 binds to vitronectin and then inhibits the interaction between the RGD site within vitronectin and endothelial cellular integrin $\alpha_v\beta_3$. PAI-1 then induces apoptosis by preventing the binding of endothelial cells to surrounding extracellular matrix during angiogenesis and disrupts integrin-mediated signaling. The resulting loss of contact then triggers the default apoptosis program within cells, called anoikis. This model is supported by results of Al Fakhri et al. (32), which showed an induced vascular apoptosis *in vitro* by the antiadhesive property of PAI-1. The antiadhesive effect is rapid *in vivo* as shown by a wave of endothelial apoptosis within 2 days of PAI-1 induction (Fig. 4A).

The same induction of endothelial apoptosis can only be recapitulated by cocultivation of TO-PAI-1 and HMEC-1 in vitronectin-coated plates but not in uncoated plates (Fig. 5). The dependence of vitronectin for PAI-1 to induce endothelial apoptosis as seen in this system lends credence to our hypothesis that the activity of PAI-1 stems in some way through disruption of endothelial adhesion to vitronectin.

The net effect of sustained tumor PAI-1 expression is long-term inhibition of tumor growth. This is likely due to a significant reduction of tumor cell proliferation as well as a slight increase in tumor apoptosis. The observation is somewhat unusual because several reports (33, 34) suggest that antiangiogenic therapy is mainly associated with tumor apoptosis. It is possible that competition between PAI-1 and cell membrane integrin already bound to vitronectin favors the latter because of its higher affinity. Once bound to its ligand, the integrin-mediated endothelial cell adhesion is further strengthened by the formation of cell-substratum focal contacts (35). During active angiogenesis and in the newly established vasculature, however, angiogenic endothelial cells actively break focal contact and further readhesion to vitronectin is inhibited by a high local concentration of PAI-1 in the tumor microenvironment. In contrast, quiescent endothelial cells statically rest on established cell-substratum contacts, which are relatively immune to PAI-1. Therefore, migrating and differentiating endothelial cells in newly established angiogenic vessels are relatively more sensitive to PAI-1 than the more well-established microvessels. Tumor growth is dependent on the continued formation of neovessels. Once interrupted, the end result is a failure to increase tumor size without necessarily shrinking the tumor, just as seen here.

Taken together, the results presented here shows for the first time the effect of PAI-1 on newly established tumor vasculature through endothelial apoptosis. This induction of endothelial apoptosis by PAI-1 has shown to be vitronectin dependent *in vitro*. The lack of endothelial apoptosis shown in previous studies may reflect the difference in experimental design with PAI-1 constitutively expressed by tumor cells or administered immediately after tumor cell implantation. Although the mechanism of endothelial apoptosis induced by PAI-1 is not clear, the data presented here suggest that PAI-1 exerts its primary effect at the early stage of tumor angiogenesis through its vitronectin-binding activity. Further experiments will exploit this finding in an attempt to enhance therapeutic modalities aimed at modulating angiogenesis.

Disclosure of Potential Conflicts of Interest

No potential conflicts of interest were disclosed.

Acknowledgments

We thank Dr. Ralph J. Bernacki for critically reading the article. Wild-type human PAI-1 cDNA was a kind gift from Dr. Daniel B. Lawrence (University of Michigan Medical School).

References

1. DeClerck YA, Imren S, Montgomery AM, Mueller BM, Reisfeld RA, Laug WE. Proteases and protease inhibitors in tumor progression. Adv Exp Med Biol 1997;425:89 – 97.

2. Stephens RW, Brunner N, Janicke F, Schmitt M. The urokinase plasminogen activator system as a target for prognostic studies in breast cancer. Breast Cancer Res Treat 1998;52:99 – 111.

3. Andreasen PA, Egelund R, Petersen HH. The plasminogen activation system in tumor growth, invasion, and metastasis. Cell Mol Life Sci 2000; 57:25 – 40.

4. Rakic JM, Maillard C, Jost M, et al. Role of plasminogen activator-plasmin system in tumor angiogenesis. Cell Mol Life Sci 2003;60:463 – 73.

5. Conese M, Blasi F. Urokinase/urokinase receptor system: internalization/degradation of urokinase-serpin complexes: mechanism and regulation. Biol Chem Hoppe-Seyler 1995;376:143 – 55.

6. Blasi F. uPA, uPAR, PAI-1: key intersection of proteolytic, adhesive and chemotactic highways? Immunol Today 1997;18:415 – 7.

7. Deng G, Curriden SA, Wang S, Rosenberg S, Loskutoff DJ. Is plasminogen activator inhibitor-1 the molecular switch that governs urokinase receptor-mediated cell adhesion and release? J Cell Biol 1996; 134:1563 – 71.

8. Stefansson S, Lawrence DA. The serpin PAI-1 inhibits cell migration by blocking integrin $\alpha_v\beta_3$ binding to vitronectin. Nature 1996;383:441 – 3.

9. Loskutoff DJ, Curriden SA, Hu G, Deng G. Regulation of cell adhesion by PAI-1. APMIS 1999;107:54 – 61.

10. Allgayer H, Heiss MM, Schildberg FW. Prognostic factors in gastric cancer. Br J Surg 1997;84:1651 – 64.

11. Berger DH. Plasmin/plasminogen system in colorectal cancer. World J Surg 2002;26:767 – 71.

12. Look MP, van Putten WLJ, Duffy MJ, et al. Pooled analysis of prognostic impact of urokinase-type plasminogen activator and its inhibitor PAI-1 in 8377 breast cancer patients. J Natl Cancer Inst 2002;94: 116 – 28.

13. Foekens JA, Peters HA, Look MP, et al. The urokinase system of plasminogen activation and prognosis in 2780 breast cancer patients. Cancer Res 2000;60:636 – 43.

14. Soff GA, Sanderowitz J, Gately S, et al. Expression of plasminogen activator inhibitor type 1 by human prostate carcinoma cells inhibits primary tumor growth, tumor-associated angiogenesis, and metastasis to lung and liver in an athymic mouse model. J Clin Invest 1995;96: 2593 – 600.

15. Bajou K, Noel A, Gerard RD, et al. Absence of host plasminogen activator inhibitor 1 prevents cancer invasion and vascularization. Nat Med 1998;4:923 – 8.

16. Bajou K, Masson V, Gerard RD, et al. The plasminogen activator inhibitor PAI-1 controls *in vivo* tumor vascularization by interaction with proteases, not vitronectin. Implications for antiangiogenic strategies. J Cell Biol 2001;152:777 – 84.

17. Gutierrez LS, Schulman A, Brito-Robinson T, Noria F, Ploplis VA, Castellino FJ. Tumor development is retarded in mice lacking the gene for urokinase-type plasminogen activator or its inhibitor, plasminogen activator inhibitor-1. Cancer Res 2000;60:5839 – 47.

18. McMahon GA, Petitclerc E, Stefansson S, et al. Plasminogen activator inhibitor-1 regulates tumor growth and angiogenesis. J Biol Chem 2001; 276:33964 – 8.

19. Stefansson S, Petitclerc E, Wong MKK, McMahon GA, Brooks PC, Lawrence DA. Inhibition of angiogenesis *in vivo* by plasminogen activator inhibitor-1. J Biol Chem 2001;276:8135 – 41.

20. Eitzman DT, Krauss JC, Shen T, Cui J, Ginsburg D. Lack of plasminogen activator inhibitor-1 effect in a transgenic mouse model of metastatic melanoma. Blood 1996;87:4718 – 22.

21. Almholt K, Nielsen BS, Frandsen TL, Brunner N, Dano K, Johnsen M. Metastasis of transgenic breast cancer in plasminogen activator inhibitor-1 gene-deficient mice. Oncogene 2003;22:4389 – 97.

22. Bergers G, Javaherian K, Lo KM, Folkman J, Hanahan D. Effects of angiogenesis inhibitors on multistage carcinogenesis in mice. Science 1999;284:808 – 12.

23. Hawighorst T, Oura H, Streit M, et al. Thrombospondin-1 selectively inhibits early-stage carcinogenesis and angiogenesis but not tumor lymphangiogenesis and lymphatic metastasis in transgenic mice. Oncogene 2002;21:7945 – 56.

24. Giavazzi R, Giuliani R, Coltrini D, et al. Modulation of tumor angiogenesis by conditional expression of fibroblast growth factor-2 affects early but not established tumors. Cancer Res 2001;61:309 – 17.

25. Yoshiji H, Harris SR, Thorgeirsson UP. Vascular endothelial growth factor is essential for initial but not continued *in vivo* growth of human breast carcinoma cells. Cancer Res 1997;57:3924 – 8.

26. Shockett P, Difilippantonio M, Hellman N, Schatz DG. A modified tetracycline-regulated system provides autoregulatory, inducible gene expression in cultured cells and transgenic mice. Proc Natl Acad Sci U S A 1995;92:6522 – 6.

27. Hebda PA, Whaley D, Kim HG, Wells A. Absence of inhibition of cutaneous wound healing in mice by oral doxycycline. Wound Repair Regen 2003;11:373 – 9.

28. Weidner N, Carroll PR, Flax J, Blumenfeld W, Folkman J. Tumor angiogenesis correlates with metastasis in invasive prostate carcinoma. Am J Pathol 1993;143:401 – 9.

29. sahi-Ozaki Y, Sato Y, Kanno T, Sata T, Katano H. Quantitative analysis of Kaposi sarcoma-associated herpesvirus (KSHV) in KSHV-associated diseases. J Infect Dis 2006;193:773 – 82.

30. Jankun J, Keck RW, Skrzypczak-Jankun E, Swiercz R. Inhibitors of urokinase reduce size of prostate cancer xenografts in severe combined immunodeficient mice. Cancer Res 1997;57:559 – 63.

31. Isogai C, Laug WE, Shimada H, et al. Plasminogen activator inhibitor-1 promotes angiogenesis by stimulating endothelial cell migration toward fibronectin. Cancer Res 2001;61:5587 – 94.

32. Al Fakhri N, Chavakis T, Schmidt-Woll T, et al. Induction of apoptosis in vascular cells by plasminogen activator inhibitor-1 and high molecular weight kininogen correlates with their anti-adhesive properties. Biol Chem 2003;384:423 – 35.

33. Li L, Wartchow CA, Danthi SN, et al. A novel antiangiogenesis therapy using an integrin antagonist or anti-Flk-1 antibody coated 90Y-labeled nanoparticles. Int J Radiat Oncol Biol Phys 2004;58: 1215 – 27.

34. Hood JD, Bednarski M, Frausto R, et al. Tumor regression by targeted gene delivery to the neovasculature. Science 2002;296:2404 – 7.

35. Stefansson S, Su EJ, Ishigami S, et al. The contributions of integrin affinity and integrin-cytoskeletal engagement in endothelial and smooth muscle cell adhesion to vitronectin. J Biol Chem 2007;282: 15679 – 89.